

# Effect of Hydroxyapatite and Titania Nanostructures on Early In Vivo Bone Response

Luiz Meirelles, DDS, PhD;\*† Lory Melin, DDS;† Timo Peltola, PhD;‡ Per Kjellin, PhD;§  
Ilkka Kangasniemi, PhD;‡ Fredrik Currie, PhD;§ Martin Andersson, PhD;§ Tomas Albrektsson, MD, PhD;†  
Ann Wennerberg, DDS, PhD;\*†

---

---

## ABSTRACT

*Purpose:* Hydroxyapatite (HA) or titania nanostructures were applied on smooth titanium implant cylinders. The aim was to investigate whether nano-HA may result in enhanced osseointegration compared to nano-titania structures.

*Materials and Methods:* Surface topography evaluation included detailed characterization of nano-size structures present at the implant surface combined with surface roughness parameters at the micro- and nanometer level of resolution. Microstructures were removed from the surface to ensure that bone response observed was dependent only on the nanotopography and/or chemistry of the surface. Early in vivo histological analyses of the bone response (4 weeks) were investigated in a rabbit model.

*Results:* In the present study, nano-titania-coated implants showed an increased coverage area and feature density, forming a homogenous layer compared to nano-HA implants. Bone contact values of the nano-titania implants showed a tendency to have a higher percentage as compared to the nano-HA implants ( $p = .1$ ).

*Conclusion:* Thus, no evidence of enhanced bone formation to nano-HA-modified implants was observed compared to nano-titania-modified implants. The presence of specific nanostructures dependent on the surface modification exhibiting different size and distribution did modulate in vivo bone response.

**KEY WORDS:** hydroxyapatite, in vivo test, nanostructures, nanotopography, osseointegration, surface modification, titania coating

---

---

Different topographical and chemical modifications of implants are currently in use to enhance bone formation to osseointegrated implants. The topographical modifications may vary from millimeter-wide grooves<sup>1</sup> to nano-size structures.<sup>2</sup> In vitro experiments have shown that cell activity may be modulated by struc-

tures on the micro- as well as on the nanoscale of resolution.<sup>3</sup> Recent efforts to develop nano-size structures for osseointegrated implants are based on size-equivalent structures present in bone, which result in a well-organized three-dimensional nanotopography.<sup>4</sup> Moreover, the biomolecules and cells involved in the early healing phase after implant installation will interact at the nanometer level.<sup>5</sup>

Reproducing the nano three-dimensional topography present in bone may improve early and long-term interaction between host bone and osseointegrated implant. Recently, an experiment on rabbits demonstrated enhanced early bone formation to implants modified with nano-hydroxyapatite (HA) structures.<sup>6</sup> However, those results may have depended on possible bioactivity/chemistry of HA and/or the topography of the implemented nano-size structures. The aim of the present study was to evaluate the bone response to nano-size HA and titania structures, that is, to investigate

---

\*Department of Prosthetic Dentistry, Institute of Odontology, Sahlgrenska Academy at Göteborg University, Göteborg, Sweden; †Department of Biomaterials, Institute of Clinical Sciences, Sahlgrenska Academy at Göteborg University, Göteborg, Sweden; ‡Turku Biomaterials Centre, University of Turku, Turku, Finland; §Department of Applied Surface Chemistry, Chalmers University of Technology, Göteborg, Sweden

Reprint requests: Luiz Meirelles, Biomaterials Department, Göteborg University, Box 412 SE405 30 Göteborg, Sweden; e-mail: luiz.meirelles@odontologi.gu.se

© 2008, Copyright the Authors  
Journal Compilation © 2008, Wiley Periodicals, Inc.

DOI 10.1111/j.1708-8208.2008.00089.x

whether nano-HA may result in enhanced osseointegration compared to nano-titania structures, in a model free of microstructures.

## MATERIALS AND METHODS

### Implants and Stabilization Plate

Cylindrical implants measuring 8 mm in length and 3.5 mm in diameter were made from commercially pure titanium rods (grade 3). Each implant had an upper threaded part screwed through a plate to achieve full fixation. The plate consisted of two side holes for the fixating screws and a threaded central hole for the implants, as previously described.<sup>7</sup> This model provides adequate fixation to the implant no matter the surface properties and has been developed to ensure maximal stability to observe microcirculation of grafted bone<sup>8</sup> and has been used in several studies.<sup>7,9</sup> The superior cylindrical part of the implant was placed underneath the plate at the cortical level of the tibia, whereas the remaining inferior part of the implant was located in the bone marrow. A total of 20 cylindrical implants were divided into two groups. One group (10 implants) was coated with nano-titania (MetAlvive™, Vivoxid, Turku, Finland) and the second group (10 implants) was modified with nanocrystalline HA (HA<sup>nanotm</sup> method, Promimic AB, Göteborg, Sweden).

### Implant Surface Modification

The titanium cylindrical implant lateral walls were ground by silicon carbide paper (4,000 grit) before coating. The apical wall of the implants was left as turned (Figure 1).

**Titania Coating.** The titania coating on titanium substrates was prepared by the sol-gel technique. Commercially available tetraisopropyl orthotitanate,  $\text{Ti}((\text{CH}_3)_2\text{CHO})_4$ , was dissolved in absolute ethanol (solution I). Ethyleneglycol monoethylether ( $\text{C}_2\text{H}_5\text{OCH}_2\text{CH}_2\text{OH}$ ), deionized water, and fuming hydrochloric acid (HCl, 37%) were dissolved in ethanol (solution II). Solutions I and II were mixed rapidly and stirred effectively (>600 rpm) for 3 minutes. The coating sol having  $\text{EtOH}:\text{Ti}(\text{OR})_4$ ,  $\text{H}_2\text{O}:\text{Ti}(\text{OR})_4$ , and  $\text{HCl}:\text{Ti}(\text{OR})_4$  molar ratios of 8.2, 1.0, and 0.018, respectively, was aged at 0°C for 24 hours before the titanium substrates were dip-coated. The sol was kept at 0°C during the dip-coating process. After 24 hours of aging, the coating was prepared by dipping the titanium sub-

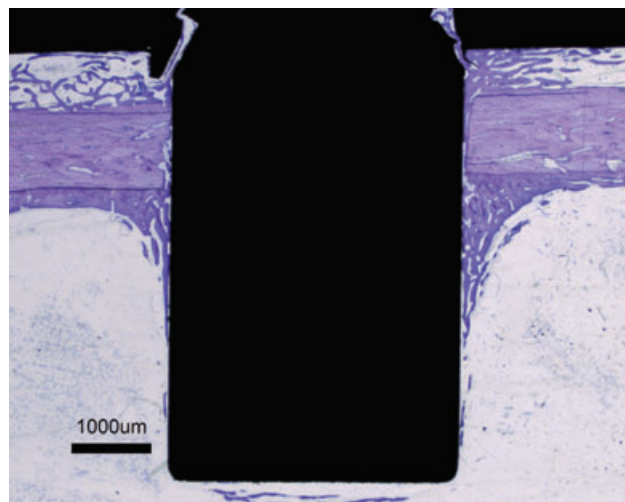


**Figure 1** Ground section stained with toluidine blue, after a healing period of 4 weeks. Bone contact was measured along the lateral (L) and apical (A) walls of the implant. Bone area measurements were calculated inside the rectangular area (·). A clear distinguishing line (\*) can be observed between original cortical bone (pale stained) and newly formed bone (dark stained). New bone formation is observed adjacent to the implant surface from the upper cortical level. New bone formation was also observed at the implant apical wall, with apparently no connection to the new bone growing from the upper or from the opposing cortex (not shown). Magnification  $\times 1$ .

strates into the sol and then withdrawing them at 0.30 mm/s. The coated substrates were heat treated at 500°C for 10 minutes. After heat treatment, the coatings were cleaned ultrasonically in acetone for 5 minutes, in ethanol for 5 minutes, and finally dried at ambient temperature. This dipping, heating, and washing cycle was repeated five times to get five subsequent layers. Finally, the materials were sterilized in an autoclave (121°C, 16 minutes, 1 bar).<sup>10</sup>

**HA Coating.** HA nanoparticles were prepared by mixing  $\text{H}_3\text{PO}_4$  and  $\text{Ca}(\text{NO}_3)_2$  with a Ca/P molar ratio of 1.67 in the presence of a liquid crystalline phase. The liquid phase is built up of surfactants, water, and a water-insoluble organic solvent. The liquid crystalline phase works as a template hindering the particle growth, that is, limits the particle size to ~5 nm. After the particles were formed, the liquid crystalline phase was dissolved, and the particles were deposited onto the titanium implants through a dip-coating technique. The dipped implant was then dried in room temperature for half an hour to evaporate any remaining organic solvent and water. Surfactants, which are adsorbed during the coating process, were subsequently burned away at

550°C for 5 minutes in nitrogen atmosphere. The method resulted in a nanocrystalline HA thin layer deposited on the implant surface.<sup>11</sup>

### Topographical Surface Characterization

Topographical analyses were performed using optical interferometry (MicroXAM™, PhaseShift, Tucson, AZ, USA) and atomic force microscopy (AFM) (Dimension 3000 SPM™, Digital Instruments, Santa Barbara, CA, USA), respectively. The optical interferometry has a lateral resolution of 0.3 μm and vertical resolution of 0.05 nm. Higher resolution evaluation of nanostructures was performed with AFM, with a lateral resolution of 2 nm and a vertical resolution at sub-nano level. At both resolutions investigated, three specimens of each type of implant were analyzed at the top, middle, and bottom parts of the lateral wall of the implant. Further, two additional measurements were performed on the apical wall of the implant.

For optical interferometry analyses, a measurement area of 200 × 260 μm (50× objective, zoom factor 0.625) was used, and a Gaussian high-pass filter (size 50 × 50 μm) was selected to remove errors of form. AFM analyses were performed in TappingMode™ using etched silicon probes (Digital Instruments) with cantilever lengths of 125 nm and resonance frequencies of 270 to 310 kHz. A measurement area of 10 × 10 μm was used and the measurements were performed at a scan rate of 1.0 Hz. Errors of tilt and bow were removed with a third-order least mean square fit (SPIP™, Image Metrology A/S, Hørsholm, Denmark). The three-dimensional roughness parameters calculated from both resolutions investigated were the arithmetic average height deviation ( $S_a$ ), the density of summits ( $S_{ds}$ ), and the developed surface ratio ( $S_{dr}$ ). Mathematical descriptions of the parameters can be found in the literature.<sup>12</sup>

The AFM measurements were further analyzed with a software processor package (SPIP, Image Metrology A/S) to characterize the surface nanostructure configuration. This software performs automatic structure identification and provides the dimension for each distinct structure. Grain analysis mode was used to identify the surface feature diameter, height, % coverage area, and number per μm<sup>2</sup>.

### Surgical Technique

Ten male New Zealand rabbits, minimally 9 months old, were used in this study. They were kept in one specially

designed room and allowed to run freely. The rabbits had free access to tap water and were fed with standard pellets, carrots, apple, and hay. The study was approved by the local animal ethical committee at Göteborg University.

Operations were performed under aseptic conditions. Animals were anesthetized with intramuscular injections of fentanyl and fluanison (Hypnorm Vet®, Janssen Pharmaceutica, Beerse Belgium) at a dose of 0.5 mL per kg of body weight, and intraperitoneal injections of diazepam (Stesolid, Dumex, Copenhagen, Denmark) at a dose of 0.25 mg per animal. If necessary, anesthesia was maintained using additional doses of Hypnorm at a dose of 0.1 mL per kg body weight. A single dose of prophylactic antibiotic (Borgal®, Intervet, Boxmeer, The Netherlands) was administered at a dose of 0.5 mL per kg body weight. All 10 animals received 0.5 mL of an analgesic (Temgesic, Reckitt and Coleman, Hull, England) at a concentration of 0.3 mg/mL on the day of operation and 3 days thereafter. Before surgery, the shaved skin of the rabbit was carefully washed with a mixture of 1% iodine and 70% ethanol. Local anesthesia with 1.0 mL of 5% lidocaine (Xylocaine®, AstraZeneca, Södertälje, Sweden) was injected subcutaneously in the surgical site. The skin and fascial layers were opened and closed separately. The periosteal layer was gently pulled away from the surgical area, and was not resutured. Three holes were drilled with a round burr on the flat proximal, medial tibial metaphysis surface parallel to the long axis of the bone. A sequence of twist drills was utilized to prepare the central hole, with a final diameter of 3.5 mm (a size that corresponded to the implant diameter) and the remaining two holes for placing the side screws. This procedure was done under copious saline irrigation at a low rotatory speed. The implant connected to the fixating plate was positioned in the central hole and fastened against the cortical bone by two side screws, as described previously.<sup>13</sup> The implant and fixating plate were already connected before surgery, and the instrument used to handle the implant–plate gripped the plate, not the implant. This ensured a safe handling of the implant by the surgeon avoiding contact with the surface.

### Histological Analyses

Four weeks after surgery, the animals were anesthetized with intramuscular injections of fentanyl and fluanison (Hypnorm Vet) at a dose of 0.5 mL per kg of body weight and further sacrificed with 10 mL overdose of

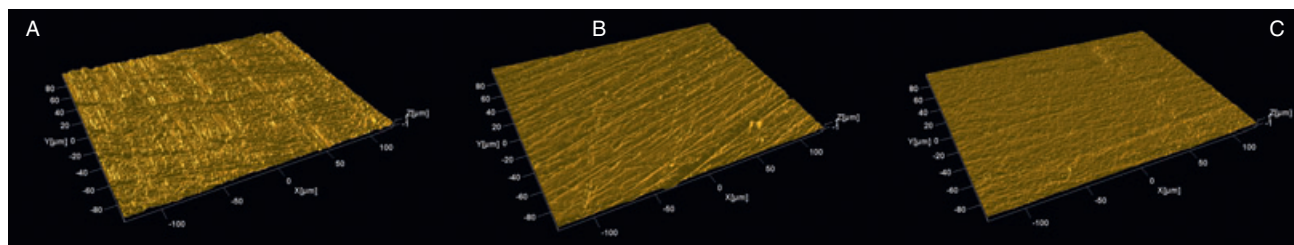


**Figure 2** Interferometer images of the polished (A), nano-hydroxyapatite (B), and nano-titania (C) implants. Measurement area of  $200 \times 260 \mu\text{m}$ .

pentobarbital 60 mg/mL, (Pentobarbitalnatrium®, Apoteksbolaget, Uppsala, Sweden). The implants with surrounding tissues were removed en bloc and immersed in 4% neutral buffered formaldehyde. Preparation of undecalcified cut and ground sections from the implants was performed with sawing and grinding equipment.<sup>14</sup> A central section was taken from each sample and ground to an approximately 40  $\mu\text{m}$  thick section and stained with toluidine blue. The amount of titanium present in each section did not allow further grinding to thinner sections. Histological evaluations were carried out using a light microscope (Eclipse ME600, Nikon, Tokyo, Japan), and histomorphometrical data were analyzed by an image analysis software (Image Analysis 2000, Tekno Optik AB, Huddinge, Sweden). Bone contact percentage was calculated on the lateral wall and apical part of the implant with  $\times 10$  objective magnification. Identification of some structures was performed if necessary with higher magnification. Bone area percentage was calculated inside a rectangle area drawn with the implant surface as base and with a height of 150  $\mu\text{m}$  as done previously on cylindrical implants<sup>13,15</sup> (see Figure 1). Measurements were made on 20 implants (10 for each group).

### Statistical Analyses

Implant insertion was randomized, and histomorphometric evaluations between the two groups were performed with the nonparametric Wilcoxon signed rank test. The significance level considered was  $p \leq .05$ .

## RESULTS

### Topographical Surface Characterization

In the lateral wall of the implants, optical interferometry images revealed a rougher surface with several parallel valleys for the polished implant (underlying topography) compared to nano-titania and -HA implants. In the nano-titania group, the valleys were extensively covered

with only few reminiscent shallow lines of the polishing step on the implant surface, which resulted in a smoother surface compared to the nano-HA implant (Figure 2). The valleys were partly covered by the nano-HA particles that resulted in a smoother appearance of the nano-HA implant compared to the polished implant surface. This indicates that the underlying topography was less modified in the nano-HA implants. Topographical evaluation of the interferometer images that suggested a decreasing surface roughness from the polished > nano-HA > nano-titania implants was ensured numerically by the surface roughness parameters calculated (Table 1).

The surface topographical evaluation at higher resolution revealed in more detail the displacement of the added nanostructures. AFM images of the nano-HA implant surface showed the valleys partly filled with some features, also present on the ridges. The valley ridge background was not present on the nano-titania implant, where the surface had a homogenous layer with the structures sitting side by side (Figure 3). The difference found in the images is in accordance with the numerical evaluation of the AFM measurements (see Table 1), where the  $S_a$  and  $S_{dr}$  surface parameters of the nano-titania were lower compared to those of the nano-HA. Following surface roughness parameter calculation, the observed features present in both implants were characterized. Features present at the surface showed decrease diameter of 24 nm ( $\pm 15$ ) and height of 1 nm ( $\pm 0$ ) for the nano-titania compared to the nano-HA implants, with a diameter of 30 nm ( $\pm 48$ ) and height of 3 nm ( $\pm 6$ ). Frequency (%) histograms of feature diameter and height are presented in Figure 4. In addition, the feature coverage area was 45% for the nano-titania and 23% for the nano-HA. The lower percentage of coverage area of the nano-HA implant, despite its larger features, is explained by the higher density (features/ $\mu\text{m}^2$ ) of 721 found in the nano-titania compared to 94 for the nano-HA implants.

**TABLE 1 Surface Topography Analyses of the Polished Implant (Not Coated), and Nano-Titania and Nano-Hydroxyapatite (HA) Coated Implants**

Implant	Interferometry			AFM			Feature Analysis			
	$S_a$ (nm)	$S_{ds}$ ( $\mu\text{m}^2$ )	$S_{dr}$ (%)	$S_a$ (nm)	$S_{ds}$ ( $\mu\text{m}^2$ )	$S_{dr}$ (%)	$n/\mu\text{m}^2$	Coverage (%)	Diameter (nm)	Z Height
	Nano-titania	121 ± 29	0.1 ± 0	1.6 ± 0.0	9.8 ± 8.0	19.7 ± 3.9	0.3 ± 0.3	721	45	24 ± 15
Nano-HA	170 ± 85	0.1 ± 0	2.6 ± 1.4	21.9 ± 6.6	18.2 ± 3.2	3.1 ± 1.0	94	23	30 ± 48	3 ± 6
Polished	225 ± 49	0.1 ± 0	5.1 ± 1.3							

Surface roughness parameters were calculated by interferometry and, at higher resolution, with atomic force microscopy (AFM). Surface feature analyses were performed on the AFM measurements.

In the apical wall of the implant (as turned), not polished with SiC (4,000) paper, interferometer analyses revealed increase surface roughness compared to the lateral wall. Comparing the two groups in the apical wall, an increase surface developed ratio ( $S_{dr}$ ) of approximately two times for the nano-titania compared to the nano-HA was observed (Table 2), whereas  $S_a$  values were slightly increased for the nano-titania compared to the nano-HA. Identical  $S_{ds}$  values were found. AFM analyses of the rougher apical wall revealed increase  $S_a$  and  $S_{dr}$  values for the nano-titania compared to nano-HA, whereas the  $S_{ds}$  showed a discrete increase for the nano-HA.

### Histological Analyses

After 4 weeks, light microscopic observations of the undecalcified ground sections revealed close contact between bone and the implant surface, with young osteocytes at a distance of 3 to 4  $\mu\text{m}$  from the implant. (Figure 5). There was a clear distinguishing line between the original cortical and the newly formed bone. At this early stage of healing, the drilling border is still present on both sides of the original cortical bone, with signs of resorption (see Figure 1). The newly formed bone was observed mainly in the endosteal region following the implant surface in the bone marrow and in the periosteal region, between the fixating plate and the original cortical bone. In addition, the newly formed bone was observed in the apical part of the implant.

The histomorphometric analyses showed bone contact of 21% (SD 10, range 5 to 33%) for nano-titania implants and 17% (SD 9, range 6 to 32%) for nano-HA implants, measured on the lateral wall of the implant. This result was not statistically significant ( $p = .1$ ). The bone contact mean values measured in the apical region demonstrated a significant increase ( $p \leq .05$ ) of 19% (SD 14, range 0 to 41%) for the nano-titania compared to 7% (SD 9%, range 0 to 29%) for the nano-HA (see Figure 5). Bone area measurements exhibited identical mean values of 48% for the nano-titania (SD 13, range 26 to 69%) and for the nano-HA implants (SD 7, range 39 to 57%) (Figure 6).

### DISCUSSION

The present study did not support enhanced bone formation to nano-HA compared to nano-titania coated implants. The implants used (in the absence of macrothreads and microstructures) ensured that the bone

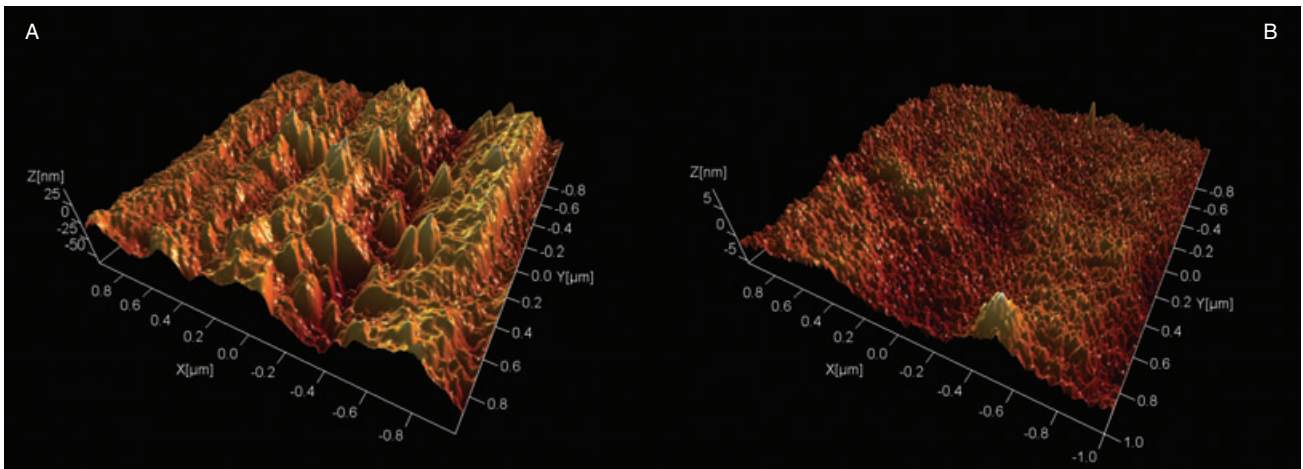


**Figure 3** Atomic force microscopy images of the nano-hydroxyapatite (A) and nano-titania (B) implants. Measurement area of  $2 \times 2 \mu\text{m}$ .

response was dependent on the nano-size structures added as well as on the surface chemistry. After 4 weeks of healing, a tendency of enhanced bone formation to nano-titania was observed compared to nano-HA-

modified implants. The beneficial chemical effect of HA seems to be of limited or no relevance in the present model. Bone response observed was modulated by the nanotopography, which was created by the implemented

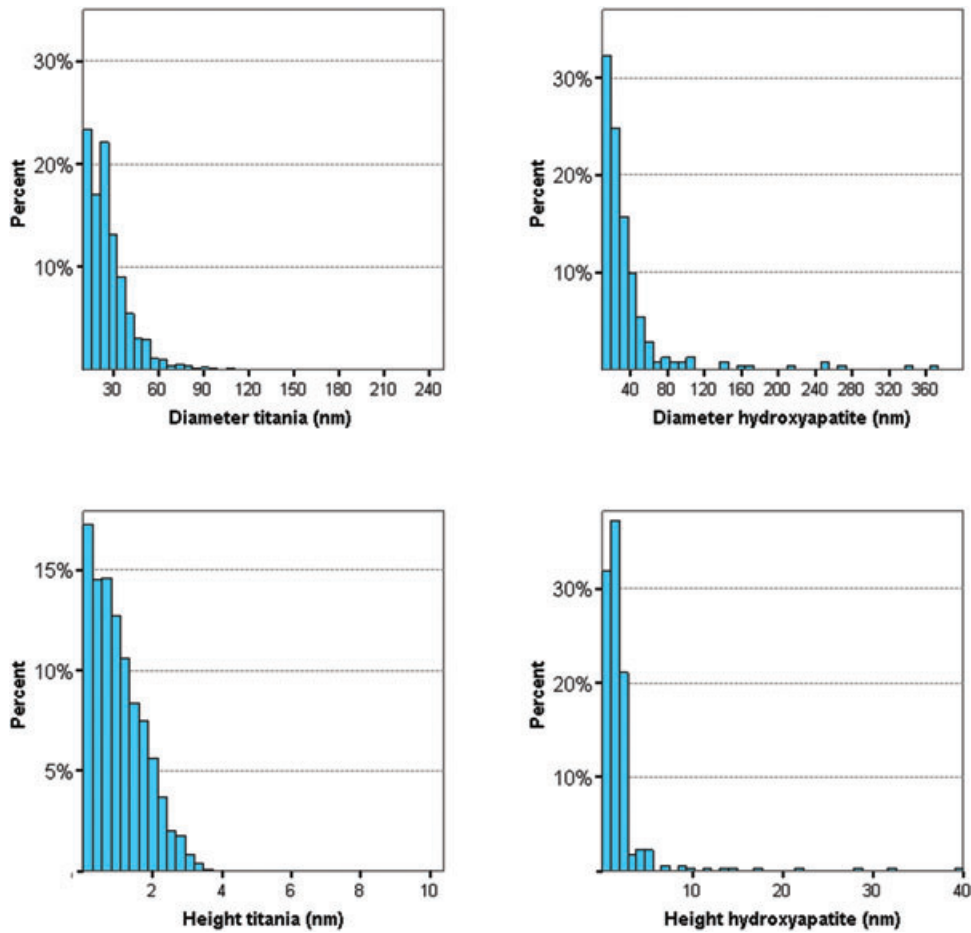


**Figure 4** Frequency histograms showing the distribution of feature diameter and height of the nano-titania and nano-hydroxyapatite implants.

**TABLE 2** Surface Topography Analysis of the Nano-Titania- and Nano-Hydroxyapatite (HA)-Coated Implants on the Apical Wall

Implant	Interferometry			AFM		
	$S_a$ (nm)	$S_{ds}$ ( $\mu\text{m}^2$ )	$S_{dr}$ (%)	$S_a$ (nm)	$S_{ds}$ ( $\mu\text{m}^2$ )	$S_{dr}$ (%)
Nano-titania	$384 \pm 29$	$0.3 \pm 0$	$19.0 \pm 3.2$	$33.8 \pm 10$	$22.7 \pm 2.1$	$5.4 \pm 1.2$
Nano-HA	$353 \pm 10$	$0.3 \pm 0$	$9.7 \pm 0.8$	$24.6 \pm 16.4$	$27.7 \pm 9.4$	$2.5 \pm 1.4$

Surface roughness parameters were calculated by interferometry and at higher resolution with atomic force microscopy (AFM).

nano-size structures. Higher resolution (AFM) evaluation revealed nano-size structures with specific dimensions and distribution at the nano-titania and -HA implants. The influence of nano-size structures on cell activity was demonstrated in the early 1990s by Clark and colleagues.<sup>16</sup> Later, results from the same group indicated that shallow grooves of 30 nm depth induced changes in cell spreading and orientation.<sup>17</sup>

Nano-titania implants had increased feature density and larger feature coverage area compared to nano-HA implants. This may represent more binding sites for protein–cell attachment and thus explain the tendency of enhanced bone contact to the nano-titania implants. Simply increasing the surface coverage area with more nano features may not ensure enhanced cell–tissue response. In an *in vitro* study with human osteoblasts, a decrease of viable cells was observed on surfaces with extreme coverage area values compared to those with intermediate values.<sup>18</sup> In addition, feature diameter and height values detected in the present study were lower for the nano-titania compared to the nano-HA implants. Furthermore, nano-titania implant surfaces demonstrated a narrow frequency histogram of the feature diameter and height, with similar values as previously reported.<sup>19</sup> Nano-HA feature diameter and height frequency histograms revealed features with larger diameter and increased height. However, the ideal feature dimensions and distribution for enhanced bone response remain unknown. Only few studies have evaluated bone cell lineage of interest to surfaces with known nano-size feature dimensions,<sup>20,21</sup> and cell activity evaluations among surfaces that possess nano features *in vitro* have not been conclusive. A clear difference is reported in cytoskeleton organization and bone cell differentiation markers when surfaces with nanotopography are compared to control – flat – surfaces.<sup>21,22</sup> Future *in vivo* experiments may elucidate the ideal feature dimension and distribution to optimize bone response to nano-modified implants.

The two methods used created not only different individual feature characteristics, but also different topographies when evaluated with AFM. Nano-titania implants exhibited an ordered arrangement forming a homogenous layer over the underlying topography, whereas nano-HA implants revealed the nano-HA features placed in a semi-ordered arrangement, not covering the entire surface (see Figure 3). The surface roughness parameters found in the present study, measured with an interferometer, showed a smooth surface ( $S_a = 120$  to  $170$  nm) for the nano-titania and -HA compared to turned ( $S_a = 0.5$   $\mu\text{m}$ ), oxidized ( $S_a = 1.0$   $\mu\text{m}$ ), and acid-etched ( $S_a = 1.5$   $\mu\text{m}$ ) implants.<sup>23</sup> The smooth values obtained at this level of resolution were crucial to the experiment design. The aim was to evaluate the effect of nanotopography on early bone response; consequently, the implant micro-roughness, known to modulate bone tissue response,<sup>24</sup> must be controlled. This was successfully achieved by a combination of the surface pretreatment (polishing) and further nano modification.

The difference of surface roughness at higher resolution (AFM) could preferentially enhance bone formation to the nano-HA implant ( $S_a \sim 22$  nm) compared to the nano-titania ( $S_a \sim 10$  nm), which could be explained by increased osteoblast adhesion mediated by specific proteins, as previously observed on surfaces with increased nano roughness parameters.<sup>25,26</sup> Interestingly, although not statistically significant, an increase of 24% in bone contact for the nano-titania (smoother) compared to nano-HA (rougher) measured on the lateral wall of the implant was observed. In addition to the tendency of enhanced bone contact on the lateral wall of the implants, isolated bone contact measured in the apical part of the implants demonstrated an increase of 170% for the nano-titania (19%) compared to the nano-HA (7%). However, the significantly higher bone response on the apical wall of the implants is explained by the surface developed area ( $S_{dr}$ ) of approximately two

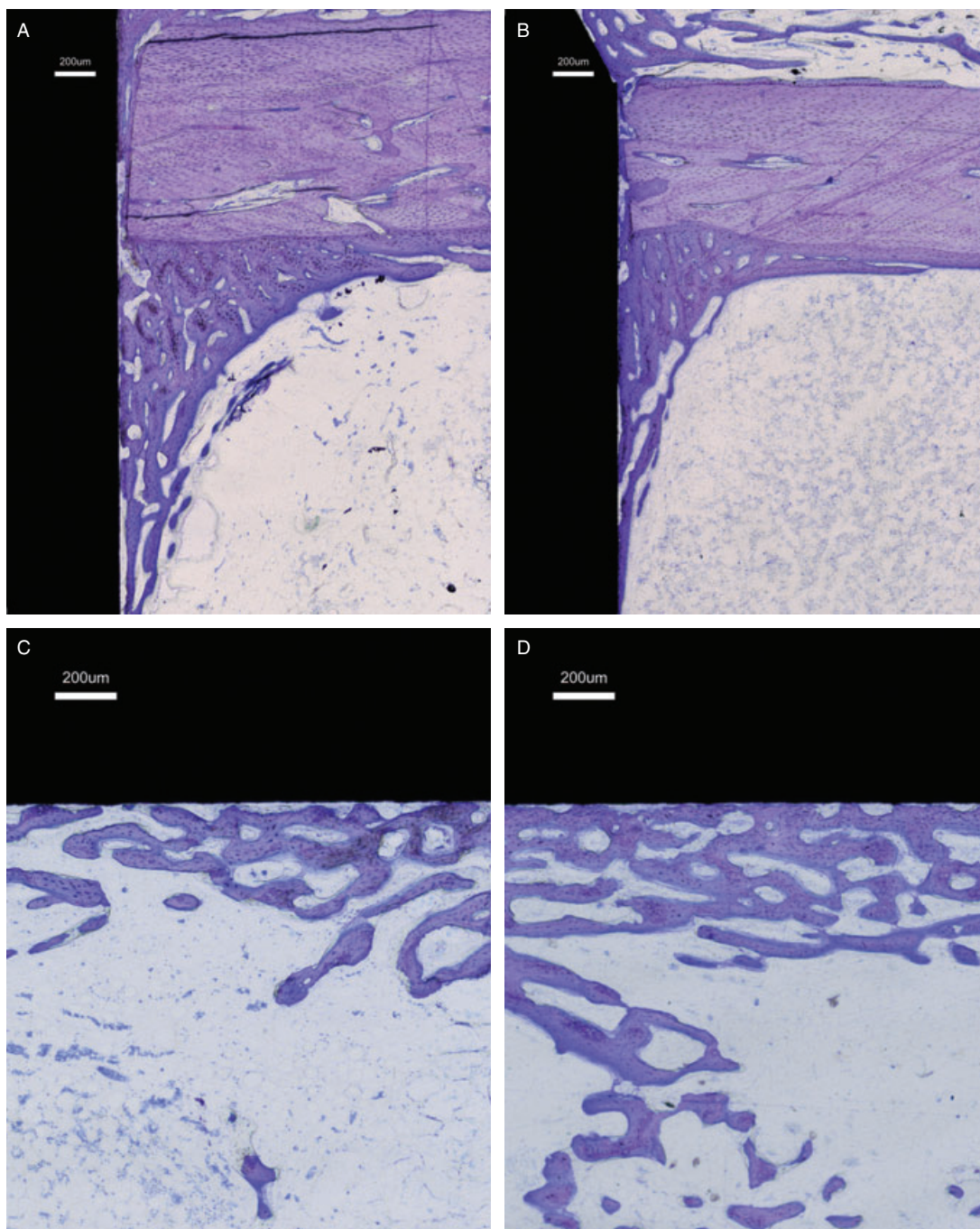


**Figure 5** Ground section ( $\times 4$ ) of the lateral (A and C) and apical (B and D) walls of the nano-hydroxyapatite and -titania implants, respectively.

times for the nano-titania compared to the nano-HA evaluated with the interferometer. This remarkable difference in the  $S_{dr}$  values was not found in the lateral polished wall.

The bone formed in the apical wall of the implant was apparently not in direct contact with preexisting bone (cortical bone). Actually, 5 mm of the implant was inside the bone marrow compartment, at a distance of

3 mm from the opposing cortex. It is not possible to affirm from where the cells were recruited to form this new bone, whether from bone marrow stem cells or from cells derived from the opposing cortex. However, the low bone formation on the lateral walls close to the implant apical part may indicate that the cells were preferentially recruited from the opposing cortex. Otherwise it is difficult to explain the discontinuity of the newly

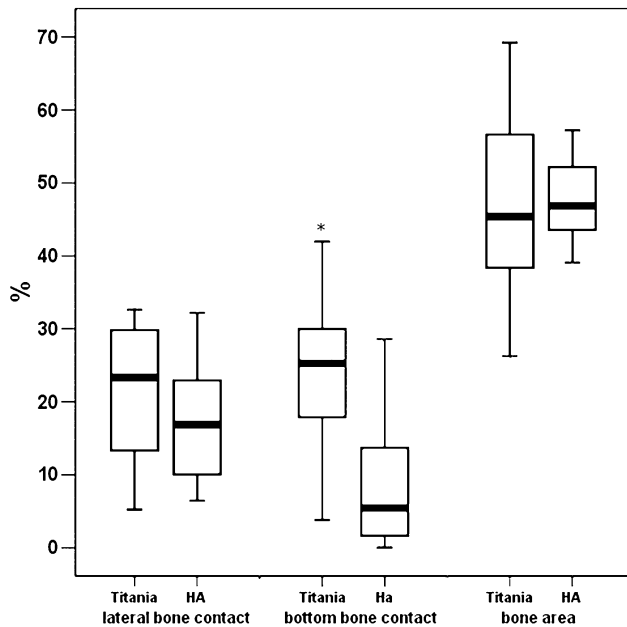


**Figure 6** Box and whisker plot of the histomorphometry analyses performed on the titania and hydroxyapatite implants. The outliers were not excluded. Wilcoxon signed rank test was selected, (\*)  $p \leq .05$ .

formed bone down growing from the upper cortical and the newly formed bone present on the apical wall of the implant, because all the implant walls were in contact with the bone marrow.

In conclusion, the enhanced bone formation to bioactive HA was not supported by the present findings. Moreover, increased surface roughness evaluated with AFM of nano-HA compared to nano-titania did not result in equivalently increased bone response, indicating that difference of surface roughness values in the nanometer level of resolution alone may not be a valuable tool to modulate response. The unexpected tendency of enhanced bone contact to the nano-titania compared to the nano-HA may be interpreted as the bone healing events at 4 weeks was dependent on the nano feature size and distribution at the surface. Future development of biomaterials with specific feature dimensions and distribution may certainly modulate tissue response and add knowledge to a better understanding of the mechanisms that lead to failure or success of osseointegrated implants.

## REFERENCES

- Hall J, Miranda-Burgos P, Sennerby L. Stimulation of directed bone growth at oxidized titanium implants by macroscopic grooves: an in vivo study. *Clin Implant Dent Relat Res* 2005; 7(Suppl 1):S76–82.
- Meirelles L, Currie F, Jacobsson M, Albrektsson T, Wennerberg A. The effect of chemical and nano topographical modifications on early stage of osseointegration. *Int J Oral Maxillofac Implants*. (In press)
- Flemming RG, Murphy CJ, Abrams GA, Goodman SL, Nealey PF. Effects of synthetic micro- and nano-structured surfaces on cell behavior. *Biomaterials* 1999; 20:573–588.
- Weiner S, Traub W. Bone structure: from angstroms to microns. *Faseb J* 1992; 6:879–885.
- Aumailley M, Gayraud B. Structure and biological activity of the extracellular matrix. *J Mol Med* 1998; 76:253–265.
- Meirelles L, Arvidsson A, Andersson M, Kjellin P, Albrektsson T, Wennerberg A. Nano hydroxyapatite structures influence early bone formation. *J Biomed Mater Res A* 2008.
- Meirelles L, Arvidsson A, Albrektsson T, Wennerberg A. Increased bone formation to unstable nano rough titanium implants. *Clin Oral Implants Res* 2007; 18:326–332.
- Albrektsson T, Albrektsson B. Microcirculation in grafted bone. A chamber technique for vital microscopy of rabbit bone transplants. *Acta Orthop Scand* 1978; 49:1–7.
- Carlsson L, Rostlund T, Albrektsson B, Albrektsson T. Implant fixation improved by close fit. Cylindrical implant–bone interface studied in rabbits. *Acta Orthop Scand* 1988; 59:272–275.
- Jokinen M, Rahiala H, Rosenholm JB, Peltola T, Kangasniemi I. Relation between aggregation and heterogeneity of obtained structure in sol–gel derived CaO–P<sub>2</sub>O<sub>5</sub>–SiO<sub>2</sub>. *Journal of Sol-Gel Science and Technology* 1998; 12:159–167.
- Kjellin P, Andersson M. SE-0401524-4, assignee. Synthetic nano-sized crystalline calcium phosphate and method of production patent SE527610. April 25, 2006.
- Stout K-J SP, Dong WP, Mainsah E, Luo N, Mathia T, Zahouani H. The development of methods for characterization of roughness in three dimensions. Birmingham: EUR 15178 EN Commission of the European Communities, University of Birmingham, 1993.
- Meirelles L, Arvidsson A, Albrektsson T, Wennerberg A. Increased bone formation to unstable nano rough titanium implants. *Clin Oral Implants Res* 2007; 18:326–332.
- Donath K. Preparation of histologic sections by cutting–grinding technique for hard tissue and other materials not suitable to be sectioned by routine methods. Norderstedt, Germany: Exakt-Kulzer Publication, 1993; 1–16.
- Hallgren C, Sawase T, Ortengren U, Wennerberg A. Histomorphometric and mechanical evaluation of the bone–tissue response to implants prepared with different orientation of surface topography. *Clin Implant Dent Relat Res* 2001; 3:194–203.
- Clark P, Connolly P, Curtis AS, Dow JA, Wilkinson CD. Cell guidance by ultrafine topography in vitro. *J Cell Sci* 1991; 99:73–77.

17. Wojciak-Stothard B, Curtis A, Monaghan W, MacDonald K, Wilkinson C. Guidance and activation of murine macrophages by nanometric scale topography. *Exp Cell Res* 1996; 223:426–435.
18. Rice JM, Hunt JA, Gallagher JA, Hanarp P, Sutherland DS, Gold J. Quantitative assessment of the response of primary derived human osteoblasts and macrophages to a range of nanotopography surfaces in a single culture model in vitro. *Biomaterials* 2003; 24:4799–4818.
19. Peltola T, Jokinen M, Rahiala H, et al. Effect of aging time of sol on structure and in vitro calcium phosphate formation of sol–gel-derived titania films. *J Biomed Mater Res* 2000; 51:200–208.
20. Riehle MO, Dalby MJ, Johnstone H, MacIntosh A, Affrossman S. Cell behaviour of rat calvaria bone cells on surfaces with random nanometric features. *Materials Science & Engineering C-Biomimetic and Supramolecular Systems* 2003; 23:337–340.
21. Dalby MJ, McCloy D, Robertson M, et al. Osteoprogenitor response to semi-ordered and random nanotopographies. *Biomaterials* 2006; 27:2980–2987.
22. de Oliveira PT, Nanci A. Nanotexturing of titanium-based surfaces upregulates expression of bone sialoprotein and osteopontin by cultured osteogenic cells. *Biomaterials* 2004; 25:403–413.
23. Arvidsson A, Sater BA, Wennerberg A. The role of functional parameters for topographical characterization of bone-anchored implants. *Clin Implant Dent Relat Res* 2006; 8:70–76.
24. Wennerberg A. On surface roughness and implant incorporation. PhD thesis, Göteborg University, Göteborg, Sweden, 1996.
25. Webster TJ, Siegel RW, Bizios R. Osteoblast adhesion on nanophase ceramics. *Biomaterials* 1999; 20:1221–1227.
26. Webster TJ, Ergun C, Doremus RH, Siegel RW, Bizios R. Specific proteins mediate enhanced osteoblast adhesion on nanophase ceramics. *J Biomed Mater Res* 2000; 51:475–483.

Copyright of Clinical Implant Dentistry & Related Research is the property of Blackwell Publishing Limited and its content may not be copied or emailed to multiple sites or posted to a listserv without the copyright holder's express written permission. However, users may print, download, or email articles for individual use.